Operation of solid oxide fuel cell on biomass product gas with tar levels >10 g Nm −3

Article *in* International Journal of Hydrogen Energy · November 2009

Impact Factor: 3.31 · DOI: 10.1016/j.ijhydene.2009.07.040

8 authors, including:

Kyriakos D Panopoulos
The Centre for Research and Technology, H…
59 PUBLICATIONS **851** CITATIONS
SEE PROFILE

Pv Aravind
Delft University of Technology
57 PUBLICATIONS **535** CITATIONS
SEE PROFILE

Marcin Siedlecki
NEX-STEP Energy Technology
12 PUBLICATIONS **154** CITATIONS
SEE PROFILE

Available at www.sciencedirect.com

ScienceDirect

journal homepage: www.elsevier.com/locate/he

Operation of solid oxide fuel cell on biomass product gas with tar levels >10 g Nm^{-3}

Ph. Hofmann[a], K.D. Panopoulos[b,*], P.V. Aravind[d], M. Siedlecki[d], A. Schweiger[c], J. Karl[c], J.P. Ouweltjes[e], E. Kakaras[a,b]

[a]Laboratory of Steam Boilers and Thermal Plants, School of Mechanical Engineering, Thermal Engineering Section, National Technical University of Athens, 9 Heroon Polytechniou Ave., Zografou, 15780 Athens, Greece
[b]Institute for Solid Fuels Technology and Applications, Centre for Research and Technology Hellas, 4th km N.R. Ptolemais-Kozani, P.O. Box 95, 50200 Ptolemais, Greece
[c]Graz University of Technology, Institute of Thermal Engineering, Inffeldgasse 25/B, 8010 Graz, Austria
[d]Delft University of Technology, Process & Energy Laboratory, Section Energy Technology, Leeghwaterstraat 44, 2628 CA Delft, The Netherlands
[e]Energy research Centre of the Netherlands ECN, Westerduinweg 3, 1755 LE Petten, The Netherlands

ARTICLE INFO

Article history:
Received 19 February 2009
Received in revised form
15 July 2009
Accepted 16 July 2009
Available online 9 October 2009

Keywords:
Solid oxide fuel cell
SOFC
Fluidized
Biomass gasification
Wood gas
Tar
Nickel gadolinium-doped ceria anode

ABSTRACT

This work assesses experimentally the feasibility of feeding a high tar load product gas from biomass gasification to a planar solid oxide fuel cell (SOFC) for renewable electricity generation. The SOFC had a nickel gadolinium-doped ceria anode (Ni-GDC) and the gasifier was a pilot scale circulating fluidized bed, employing hot gas-cleaning to remove particulates, HCl and H_2S. The SOFC operated for several hours on either pre-reformed gas (reduced tar levels < 0.5 g Nm^{-3}) as well as on high tar-laden wood gas (tar levels > 10 g Nm^{-3}) i.e. with no pre-reforming of tars. The tests were carried out at low fuel utilization U_f of around 20% at a current density $j = 130$ mA cm^{-2}. In all cases stable continuous SOFC performance was established. Post experimental examination of the SOFC showed that the anode was not affected by carbon deposition or other impurity accumulation.

1. Introduction

Ligno-cellulosic biomass is a renewable energy source that can be converted via thermochemical gasification into a gaseous mixture rich in H_2, CO, CH_4 as well as CO_2, N_2 and H_2O, in proportions depending on the gasification technique applied. The product gas also contains trace constituents: particulates, H_2S, NH_3, HCN, corrosive volatile alkali or metal compounds that escape from high temperature gas cleaning, and tars which are a complex mixture of organic compounds

* *Corresponding author*. Tel.: + 30 210 6501771; fax: + 30 210 6501598.
E-mail address: panopoulos@certh.gr (K.D. Panopoulos).
0360-3199/$ – see front matter © 2009 Professor T. Nejat Veziroglu. Published by Elsevier Ltd. All rights reserved.
doi:10.1016/j.ijhydene.2009.07.040

mostly of aromatic nature that derive from the biomass pyrolysis products and secondary reactions [1]. These are considered contaminants and must be removed to proper levels according to specifications of the downstream application, such as for power production. Conventionally such applications can be an internal combustion engine or a gas turbine combined cycle.

High temperature fuel cells, such as the SOFC, can utilise the major product gas combustible contents (H_2, CO and CH_4) to produce power efficiently, as well as high quality thermal energy from their off gas which can be further used in gas turbines or for system integration and/or process heating purposes. SOFCs are considered the most tolerant fuel cell type to several fuel gas impurities, such as H_2S [2]. Nevertheless, SOFC tolerance towards the other trace constituents of biomass derived product gas is not well investigated yet and therefore it remains unclear if operation on product gas is feasible. In principle (a) particulates of ash and non-converted char could deposit on SOFC anodes and result in blocking of gas diffusion paths or (electro-) catalytically active sites as well as in detrimental carbon formation, (b) H_2S can temporarily or permanently poison nickel containing anodes at reported levels from 1 ppmv [2] up to 240 ppmv [3] (c) HCl was reported not to have a significant impact at levels of 9 ppmv [4] (d) while NH_3 is reported to be a fuel without degradation effect [5]. The rest of the impurities are scarcely documented for their effect on SOFC operation: (e) volatile alkali compounds and (f) tars. It has been proven thermodynamically that under certain fuel conditions tars could induce carbon deposition on Ni containing anodes [6]. In practice, deriving from the well studied methane steam-reforming on Ni-based catalysts, operation with high S/C (the molar ratio of steam to carbon) of above 2.5 [7] is recommended to avoid carbon deposition in SOFC systems, but required steam production to achieve this can lead to overall system efficiency penalties. Therefore a more effective solution is to employ anode materials with higher resistance against carbon deposition, such as Ni-GDC based cermets. Several works have proven its stable operation on weakly humidified methane [8] because of its ability to transform carbon deposits to CO or CO_2 during or after CH_4 decomposition through the cermets mobile bulk lattice oxygen content [9,10].

Most of the experimental works published on the SOFC and biomass gasification integration have used mixtures of synthetic gases to emulate product gas expected compositions [11]. Baron et al. [12] performed such tests at intermediate operating temperature ($T = 650$ °C) with Ni-GDC anodes and found that CH_4 up to 10% with $S/C = 1$ resulted in poor power output due to carbon deposition while Ouweltjes et al. [13] tested with S/C as low as 0.8 and $T = 850$–920 °C (i.e carbon deposition not predicted by thermodynamics), with the inclusion of H_2S up to 9 ppmv, which caused deactivation of the anode towards methane reforming but did neither affect H_2 nor CO electrochemical oxidation. Synthetic gas tests carried out by Dekker et al. [14] revealed that lighter hydrocarbons such as acetylene and ethylene as well lighter tar compounds such as toluene did not affect the cell operation, but the introduction of low concentrations of heavier hydrocarbons such as naphthalene, phenanthrene and pyrene caused a strong reduction of internal methane reforming resulting in voltage degradation. Aravind et al. [4] reported emulated product gas tests including 628 mg Nm^{-3} of naphthalene without observing significant impact on SOFC performance. Using real biomass derived gas as SOFC feed, Oudhuis et al. [15] coupled a two stage gasifier to a downscaled 'state of the art' Sulzer HEXIS stack for a duration of 48 h, showing that the principle works but observed soot formation during fuel heating which negatively influenced the cell performance. Similarly, Nagel et al. [16] operated a 1 kW Hexis stack with gas from an updraft wood gasifier (tar load approx. 8 g Nm^{-3}) observing a performance loss of 6% within 30 h of operation. The same type Ni-GDC anode SOFC as employed in this presented work ran successfully for 150 h on a tar-free cold-cleaned wood gas from a two-stage fixed-bed downdraft gasifier with a low $S/C = 0.5$ [17]. Furthermore, successful SOFC tests on tar laden wood gas from other gasification facilities were presented in [18].

In this paper part of the results obtained within the EU project BioCellUS [19] (Biomass fuel Cell Utility System) are presented. More specifically the results concern the successful short-term operation of a single planar Ni-GDC anode SOFC on hot-cleaned producer gas from a circulating fluidized bed biomass gasifier. The SOFC was operated on pre-reformed quality wood gas (<0.5 g Nm^{-3} tars) as well as on high tar-laden wood gas (>10 g Nm^{-3}).

2. Experimental

A slipstream from the product gas of the 100 kW_{th} atmospheric circulating fluidized bed gasifier (ACFBG) located at Delft University of Technology – Process and Energy Department, was processed in a gas-cleaning and conditioning unit (GCU) and subsequently delivered as fuel gas to a mobile planar unsealed SOFC test facility, either (a) reformed or (b) non-reformed and thus containing high tar levels. A schematic of the experimental set-ups is shown in Fig. 1 and comprises three sections described hereafter, followed by a summary of the experimental characteristics and procedure.

2.1. 100 kW_{th} atmospheric circulating fluidized bed gasifier (ACFBG) test rig

The gasification experiments have been carried out on an atmospheric 100 kW_{th} Circulating Fluidized Bed Gasifier [20]. A schematic drawing of the test rig is presented in Fig. 1 (section a). The main characteristics of the rig are: riser length of 5.5 meters, riser inner diameter of 83 mm, downcomer inner diameter of 54 mm, fluidization medium preheater (6 kW), electrical trace heating of the whole rig (22 kW), high temperature ceramic filter unit (BWF) operating at 450 °C, and feeding system able to supply biomass at a maximum rate of 20 kg h^{-1}. The feeding location used during the experiments described here is located 900 mm above the gas distribution plate. A mixture of steam and oxygen was used as fluidization and gasification medium. The measurement equipment consists of mass flow meters and controllers for all input streams, thermocouples (K-type), (differential) pressure

meters, weighing devices, and a volume flow meter for the product gas. The composition of the produced gas was analysed using the equipment connected just upstream the filter unit. The analysed gas components were: CO_2, CO by means of NDIR online analysers, O_2 using paramagnetic analyser, H_2, N_2, CH_4, CO, CO_2 by means of a micro GC (response time 180 s), CO_2, CO, CH_4, C_2H_4, C_2H_2 by means of FTIR spectrometer (offline). Water has been measured gravimetrically. Tar measurements have been done using the SPA method, developed at KTH [21].

The bed material used during this experimental campaign was silica sand; the mean particle size of the bed material was approximately 386 μm. The gasified solid fuel was in this case clean wood pellets (A quality wood). The original pellet size was 6 mm in diameter, ground down to ~3 mm to eliminate internal recirculation problems of the solids in the CFB.

2.2. Gas cleaning and conditioning & gas analytics

Fig. 1 (section b) shows the main features of the gas conditioning unit (GCU), described in detail in [18,22]. First, particulates are removed from the gas in two steps (hot gas cyclone and sinter metal filter candle). With the help of an ejector pump using pressurized steam as the actuating fluid, the atmospheric product gas slipstream from the ACFBG was induced to a higher pressure level in order to overcome subsequent pressure losses in the trace constituents trap beds. These were firstly a chlorine removal bed (sodium

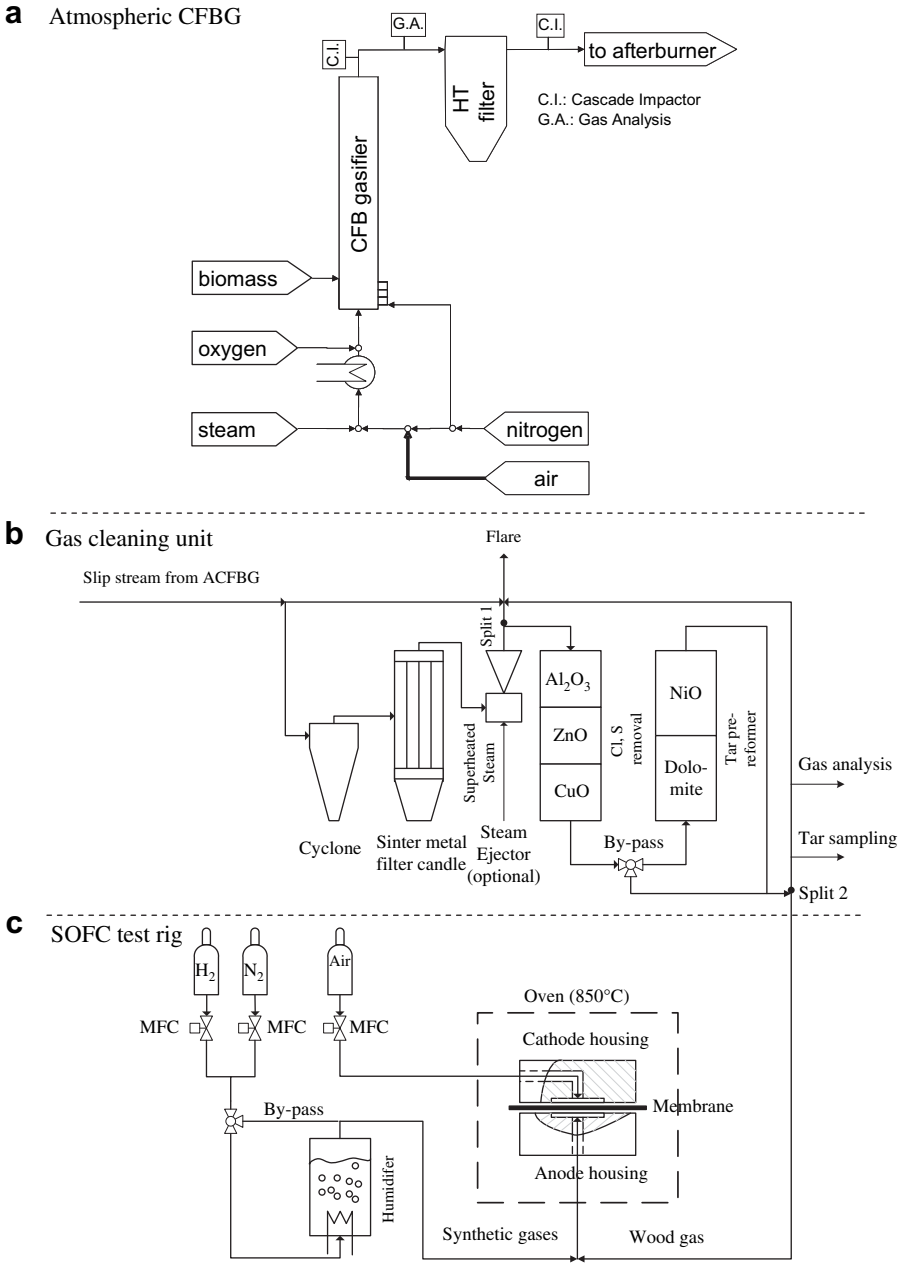

Fig. 1 – a) 100 kW_{th} atmospheric circulating fluidized bed gasifier (ACFBG), b) gas cleaning and conditioning unit (GCU) and c) SOFC test rig.

promoted alumina), a 2-step H_2S removal (ZnO and ZnO/CuO beds) and finally a 2-step tar reformer (dolomite and NiO beds). The tar reformer could be by-passed thus allowing the tar to reach the SOFC.

Split flow fractions of the product gas were used to on-line measure the dry permanent species composition using an ABB™ analyser with a NDIR detector (URAS14) for CO, CH_4, and CO_2, a paramagnetic detector for O_2 and a TCD (CALDOS) for the H_2 content. The balance difference (not measured) constitutes mostly product gas N_2 and to a lesser extent light hydrocarbons (e.g. C_2H_x, C_3H_x) [23]. The steam content was measured both gravimetrically (periodically) and with a psychrometric H_2O sensor (semi on-line). The H_2S concentration was on-line measured with a colorimetric instrument (lead acetate) from SICK MAIHAK (MONOCOLOR 1N) and validated with DRAEGER.

To determine the tar load of the wood gas fuelling the SOFC, several tar samplings according to the tar protocol (TP) [24] as well as solid-phase-adsorption (S.P.A.) method [21] were performed from a sample line installed directly before the wood gas feed line entering the SOFC test rig, in order to assure that the evaluated tar loads represented a good estimation of the tar levels that actually reached the SOFC anode. The SOFC feed gas line was trace heated to above 400 °C to prevent tar condensation and carbon formation prior to the SOFC. The gas lines were checked for carbon or tar deposits after each test by thoroughly washing them with iso-propanol, however no mentionable line contamination was detected.

The on-line measurement of the hot wood gas flow throughput to the SOFC was achieved by measuring the differential pressure over orifices (evaluating the flow together with data from the on-line gas analysis). The flow control was performed by adjusting the back pressure of the GCU and taking into account the employed gas splitting ratios.

2.3. SOFC test rig and membranes employed

A schematic of the SOFC single-cell test rig together with its peripheral equipment is shown in Fig. 1 (section c). The cell housing and anode/cathode gas tubes are placed inside a temperature controlled oven. The cell housing is made of two Al_2O_3 flanges with channels for gas distribution, and spot welded current collectors (platinum gauze for cathode and nickel gauze for the anode). The housing is seal-less, therefore depleted gases burn outside the cell. The cell temperature is measured at the centre, where anode and cathode gases enter. The voltage–current (V–j) characteristics (polarization curves) were measured with a variable electronic load (PLZ 664WA Kikusui Electronics Corp, Japan), supported by an additional power supply unit (SM120-25D Delta Elektronica, Zierikzee, Netherlands) in order to compensate for the low cell voltage. All collected signals were logged in a data acquisition system.

In order to condition the SOFC anode and allow an overnight interruption of wood gas operation, mixtures of H_2 and N_2 were provided from bottles and flows adjusted with mass flow controllers while the level of humidification was achieved by passing the gas mixture through a water bubbler operated at room temperature.

The experiments were performed with a circular shaped planar electrolyte-supported SOFC membrane manufactured by InDEC B.V., consisting of a nickel/gadolinium-doped ceria (Ni-GDC) anode, yttrium stabilised zirconium oxide (YSZ) electrolyte and a strontium doped lanthanum manganite (LSM) cathode, with a diameter of 120 mm and an active surface area of $A = 100\ cm^2$. The cell's main features are summarised in Table 1.

2.4. Experimental characteristics and procedure

The SOFC was first tested on an almost tar-free wood gas (phase **a**), employing the tar reformer of the GCU. Then the reformer was by-passed allowing the tar load to reach the cell (phase **b**). Overnight the SOFC operation was put on humidified hydrogen/nitrogen (bottled gases) operation and the experiment continued the following day again on full tar load (phase **c**).

The SOFC fuel utilization factor U_f, describing the extent of electrochemical reactions via Eq. (1), was determined on-line by operating the SOFC in galvanostatic mode with a set current $I = 13$ A (corresponding to current density $j = 130\ mA\ cm^{-2}$) and monitoring the inlet wood gas flow and composition. The fuel utilization was deliberately kept low, in the range of 20%, in order to prevent deteriorating nickel oxidation in the anode in case of fuel shortages due to unstable wood gas supply or potential loss of methane reforming activity. It was calculated from the following equation:

$$U_f = \frac{I}{2 \cdot F \cdot \dot{n}_f \left(x_{H_2} + x_{CO} + 4 \cdot x_{CH_4}\right)} \quad (1)$$

where $\dot{n}_f$ is the anode mole flow, F is Faraday's constant and x_i the input mole fractions of combustible gases, taking into account that CO can produce an extra H_2 through the water gas shift (WGS) reaction, while CH_4 can produce 4 additional H_2 through its reforming and WGS of the produced CO. Both hydrocarbons higher to methane and tars were neglected in this calculation; thus the calculation is expressed in a conservative manner. The current I (in A) is expressed through Faraday's law:

$$I = 2 \cdot F \cdot \dot{r}_{H_2} \quad (2)$$

assuming that hydrogen is the only electrochemical active species with its reaction rate $\dot{r}_{H_2}$. The SOFC operating temperature was set to 850 °C, measured at the fuel inlet which is situated at the centre of the cell.

Table 1 – Planar SOFC dimensions and materials.

	Thickness [μm]	Layer/Composition
Anode	40	Current collecting Ni Functional Ni and $Gd_{0.1}Ce_{0.9}O_2$ Contact $Gd_{0.4}Ce_{0.6}O_2$
Electrolyte	90	$Y_{0.06}Zr_{0.94}O_2$
Cathode	40	Functional $La_{0.75}Sr_{0.2}MnO_3$ and $Y_{0.16}Zr_{0.84}O_2$ Current collecting $La_{0.75}Sr_{0.2}MnO_3$

The procedures for cell heating, reduction and conditioning prior to wood gas operation as well as the cooling procedure are described in detail in [17,18]. The first 0.5–1 h on wood gas were operated at open-circuit voltage (OCV), i.e. with no current load, in order to allow the cell to reach a new steady-state. Cell performance loss was investigated by comparing V–j curves measured on a H_2/N_2 reference gas mixture before and after wood gas operation.

All anode gas mixtures outside wood gas operation were humidified at room temperature (approx. 2–3 vol-% H_2O depending on the room temperature). A slightly reducing atmosphere was sustained on the anode side during the cool-down procedure to prevent the re-oxidation of nickel. Bottled pure gases of laboratory standard 5.0 were used for N_2, H_2 and synthetic air (80 vol-% N_2, 20 vol-% O_2).

After the testing the SOFC membrane was examined extensively with Scanning Electron Microscopy (SEM) and Energy Dispersive Spectrometry (EDS) to determine any carbon deposition on the anode structure, contamination of traces or anode structure alteration. For comparison reasons an identical SOFC membrane was solely used on a reference H_2/N_2 350/450 Nml min^{-1} anode mixture humidified at room temperature, and cathode synthetic air flow of 2000 Nml min^{-1}.

3. Results and discussion

An overview of the three test phases is given in Table 2, presenting average experimental operational parameters concerning measured and derived values during the SOFC current load operation on wood gas.

Table 2 – Conditioned wood gas and SOFC operation characteristics (averaged values).

Test phase		a	b	c
Operation on real wood gas [h]		2.5	1	7
Tars [g Nm^{-3}]		~0	>10	>10
H_2S [ppmv]		0.14	0.27	0.40
Main wood gas composition				
x_{H_2}	vol-%	23.9	4.0	4.1
x_{CO}		2.6	7.5	8.0
x_{CH_4}		0.3	2.0	2.0
x_{CO_2}		13.8	5.0	5.4
x_{N_2} + rest[a]		5.3	8.5	7.4
x_{H_2O}		54.1	73.0	73.1
Measured SOFC parameters				
Cell voltage, V_{cell}	[mV]	811	787	788
Current density, J	[mA cm^{-2}]	130	130	130
Cell temperature, T_{cell}	[°C]	853	839	848
Anode (fuel) flow, $\dot{Q}_f$	[Nml min^{-1}]	2009	2049	2039
Cathode flow, $\dot{Q}_c$	[Nml min^{-1}]	2000	2000	2000
Derived parameters				
Lower heating value, *LHV*	[MJ Nm^{-3}]	3.0	2.1	2.2
Fuel utilization, U_f	[%]	17.0	23.3	22.4
Oxygen utilization, U_{O_2}	[%]	11.4	11.4	11.4
Electrical efficiency, η_{el}	[%]	10.5	14.3	13.7

a C_2H_x, C_3H_x, etc. which in case of the reforming (phase a) were most likely reformed

3.1. Main gas composition

During the tests described in this paper, the ACFBG was operated at an equivalence ratio (λ) of around 0.23 and a steam-to-biomass ratio (SB) of around 0.90. The gas produced had the following representative average gas composition: H_2 14.0%, CO 28.6%, CO_2 17.2%, CH_4 7.2%, C_2H_4 2.1%, N_2 22.9% (vol-%, dry basis). The measured moisture content of the raw gas was around 50–60 vol-%.

The average main gas composition of the wood gas after the addition of steam from the ejector, measured before entering the SOFC, is given in Table 2. Its course and its lower heating value (LHV) are presented in Fig. 2 for all three test phases. For operation with the reformer (phase **a**: duration ~2.5 h), an upward trend for H_2O and a downward trend for H_2 content resulted in a slightly decreasing LHV with an average around 3 MJ Nm^{-3}. The non-reformed wood gas fuelling the SOFC during phases **b** (duration ~1 h) & **c** (duration ~7 h) was leaner due to the missing steam reforming energy with a lower LHV at around 2 MJ Nm^{-3}; the course of the gas composition was rather stable.

Although some light hydrocarbons were measured at the gasifier outlet, these compounds are not included in the following SOFC performance evaluation since they were not measured after the GCU, and thus the fate of them could not be determined.

The SOFC anodic atomic gas composition for the whole range of tests at OCV and at the cell's exit under current load is plotted in the C–H–O ternary phase diagram of Fig. 3 and proves safe operation away from the thermodynamically predicted solid carbon $C_{(s)}$ and $NiO_{(s)}$ regions. The phase boundary lines for solid carbon $C_{(s)}$ and $NiO_{(s)}$ at 850 °C were generated with the Phase Diagram module of FactSage™ software [25].

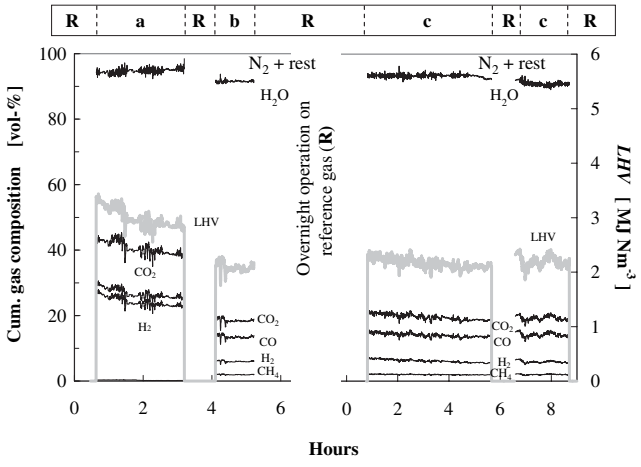

Fig. 2 – a) Wood gas main gas composition (cumulative) fuelling the SOFC and its LHV vs. time for all three test phases indicated above by a, b and c (R indicates operation on the H_2/N_2 reference gas mixture).

3.2. H_2S course and breakthrough

H_2S breakthrough occurred during test phase **b** reaching 0.3 ppmv, and during test phase **c** the breakthrough started at approximately 0.2 ppmv and increased within the final test hour to 1.25 ppmv as presented in Fig. 4.

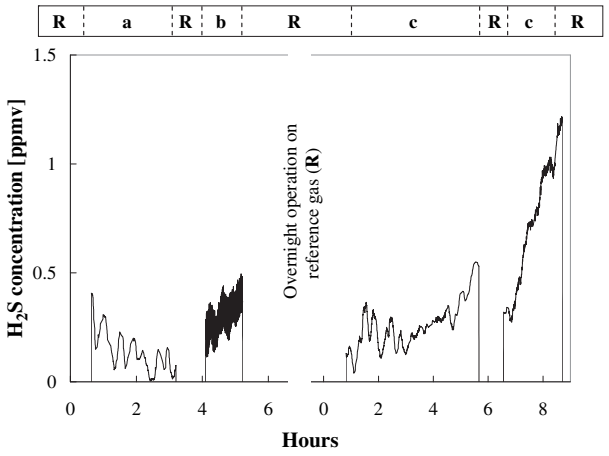

Fig. 4 – H_2S concentration (in ppmv) vs. time for all three test phases indicated above by a, b and c (R indicates operation on the H_2/N_2 reference gas mixture).

3.3. Tar measurements

The results of the tar samplings of the wood gas before entering the SOFC are listed in Table 3. For the reformed gas (phase **a**), tars in the range of 100–500 mg Nm^{-3} slipped through to the cell while the non-reformed wood gas (phases **b** and **c**) contained a tar load of greater than 10 g Nm^{-3} which actually reached the SOFC anode during operation. Gas chromatography analysis of the sampled tars revealed a lot of different tar species among which compounds such as Benzene (~12–13 g Nm^{-3}), Toluene (~3 g Nm^{-3}), Phenol (~2 g Nm^{-3}), o-Xylene and Styrene (~0.3–1.8 g Nm^{-3}), Indene (~1–2.5 g Nm^{-3}), Naphthalene (~3–5 g Nm^{-3}) and Phenanthrene (~0.5–1 g Nm^{-3}) were most abundant with concentrations >1 g Nm^{-3}. Rather large differences between the three tar analysis methods occurred: while the gravimetrically determined total tar concentrations from the tar protocol samplings (~10.5 g Nm^{-3}) fall close to the total tar concentrations determined by the S.P.A. method (~11.1 g Nm^{-3}), the GC analysis of the tar protocol samples resulted in much higher values. Part of the difference can be attributed to benzene and toluene, which were not detected by the S.P.A. method and which most likely were evaporated during the preparation for the gravimetric analysis which involves an evaporation of the trapping solution (iso-propanol). The gravimetrically determined tar concentration is regarded as the minimum amount of tars which reached the SOFC anode during wood gas operation and the including of major species such as benzene and toluene is an issue of definition of the ''tar content''.

3.4. SOFC performance results

Overall, the SOFC voltage output during current load of 13 A (≡130 mA cm^{-2}) followed a stable course for all three test phases as shown in Fig. 5 with the fluctuations arising from the gasifier process inherent gas composition instability. The fuel utilization was stable with respective average values for the three test phases of 17%, 23.3% and 22.4% ensuring that the SOFC was operated in a safe area, where no risk of anode oxidation was present.

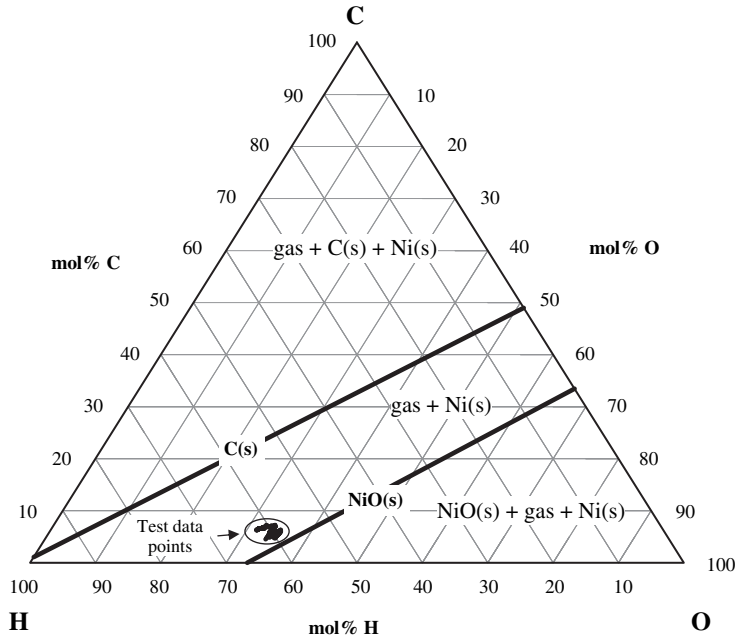

Fig. 3 – C–H–O ternary phase diagram with thermodynamic equilibrium prediction lines for $C_{(s)}$ and $NiO_{(s)}$ at 850 °C and plotted points corresponding to the anodic cell's exit gas composition during all three test phases.

Table 3 – Tar analysis results (composition in mg Nm^{-3}) from tar protocol (gravimetric and GC) and S.P.A. method (GC) measurements.

Phase		a		b			c		
Class	Species	Method/sample							
		TP/1	TP/2	SPA/1	SPA/2	TP/3	TP/3	SPA/3	SPA/4
2	Phenol	1.28	0.58	13.8	1756.1	2126.02	2387.19	1810.1	2051.2
2	o-Cresol	0.11	0.00	0.0	56.7	131.40	126.35	42.9	50.9
2	m/p-Cresol	0.19	0.08	0.0	261.4	336.19	362.33	256.5	287.3
2	Quinoline	0.00	0.00			26.83	28.37		
2	Isoquinoline	0.00	0.00			8.90	10.06		
	Class 2 total	**1.58**	**0.66**	**13.8**	**2074.2**	**2629.34**	**2914.3**	**2109.5**	**2389.4**
3	Toluene	1.32	0.80	152.1	146.0	3207.51	2982.34	179.8	116.5
3	Ethylbenzene	0.17	0.09			148.98	102.01		
3	m/p-Xylene	0.00	0.00	0.0	7.2	233.85	213.78	7.0	0.0
3	o-Xylene + Styrene	0.62	0.36	63.3	320.8	1757.23	1751.94	395.1	281.4
	Class 3 total	**2.11**	**1.25**	**215.4**	**474**	**5347.57**	**5050.07**	**581.9**	**397.9**
4	Indene	1.07	0.68	16.1	1072.0	2516.15	2467.73	1247.0	900.2
4	Naphthalene	2.38	1.31	78.6	3173.3	4842.88	4849.49	3352.8	3125.4
4	2-methylnaphthalene	0.28	0.15	112.4	543.8	547.67	534.98	520.2	534.7
4	1-methylnaphthalene	0.20	0.00	5.5	235.9	389.97	379.26	221.8	248.5
4	Biphenyl	0.18	0.00	0.0	432.3	343.28	346.16	440.9	464.4
4	Ethenylnaphthalene	0.00	0.00	–	–	175.82	205.25	–	–
4	Acenaphthylene	0.30	0.00	0.0	551.0	839.84	999.17	383.8	635.8
4	Acenaphthene	0.46	0.20	0.0	236.8	780.56	636.30	244.7	266.0
4	Fluorene	0.16	0.00	11.0	242.0	489.55	471.07	214.9	237.7
4	Phenanthrene	0.57	0.33	0.0	512.2	977.99	956.99	490.3	567.1
4	Anthracene	0.23	0.00	0.0	285.1	331.10	325.08	287.0	309.5
	Class 4 total	**5.83**	**2.67**	**223.6**	**7284.4**	**12234.81**	**12171.48**	**7403.4**	**7289.3**
5	Fluoranthene	0.00	0.00	0.0	415.5	342.22	331.99	406.9	426.4
5	Pyrene	0.00	0.00	0.0	375.2	418.72	419.91	328.9	386.4
5	Benzo(a)-anthracene	0.07	0.00			135.96	133.66		
5	Chrysene	0.00	0.00			81.88	74.81		
5	Benzo(b)-fluoranthene	0.00	0.00			68.68	68.96		
5	Benzo(k)-fluoranthene	0.03	0.00			22.39	21.15		
5	Benzo(e)-pyrene	0.00	0.00			22.98	25.48		
5	Benzo(a)-pyrene	0.00	0.00			55.62	57.60		
5	Perylene	0.00	0.00			5.30	5.95		
5	Indeno(1,2,3-cd)-perylene	0.00	0.00			24.44	26.02		
5	Dibenz(a,h)-anthracene	0.00	0.00			0.00	0.00		
5	Benzo(g,h,i)-perylene	0.00	0.00			11.16	11.83		
5	Coronene	0.00	0.00			0.00	5.30		
	Class 5 total	**0.1**	**0**	**0**	**790.7**	**1189.35**	**1182.66**	**735.8**	**812.8**
B	**Benzene**	4.82	2.53			13326.48	12270.09		
I	**Indan**			13.5	0.0			0.0	0.0
X	**2,4-Xylenol**			0.0	282.1			425.0	331.7
U	Unknowns-1[a]	3.91	4.97			1729.75	1830.55		
U	Unknowns-2[b]	1.23	1.24			2417.18	2496.30		
U	Unknowns-3[c]	0.34	0.00			1088.53	1072.47		
U	Unknowns-4[d]	0.88	0.00			771.21	879.80		
U	Unknowns-5[e]	0.00	0.00			34.71	57.06		
U	**Unknowns total**	**6.36**	**6.21**			**6041.38**	**6336.18**		
	GC total	**20.8**	**13.32**	**466.3**	**10905.4**	**40768.93**	**39924.78**	**11255.6**	**11221.1**
	Gravimetric tar	**77.68**	**111.74**			**10959.19**	**9923.52**		

a Benzene t/m naphthalene.
b Naphthalene t/m phenantrene.
c Phenantrene t/m pyrene.
d Pyrene t/m benzo(e)pyrene.
e Benzo(e)pyrene t/m coronene.

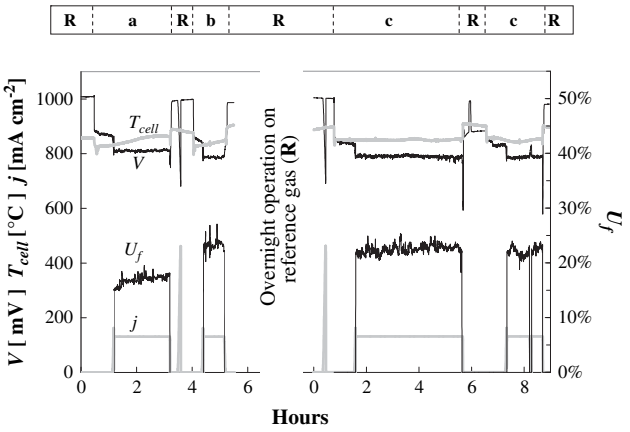

Fig. 5 – Cell voltage V, temperature T_{cell}, current density j and fuel utilization U_f vs. time for all three test phases indicated above by a, b and c (R indicates operation on the H_2/N_2 reference gas mixture).

During phase **a**, the first 0.5 hours were operated on open-circuit voltage (OCV) which was slightly decreasing before approaching steady-state (~870 mV). Subsequently, the SOFC was operated for ~2 h at 130 mA cm^{-2} on the pre-reformed wood gas with a resulting cell voltage of around 810 mV. After 1 h operation on the synthetic reference gas mixture (phases **R**), the SOFC was fueled again with wood gas, this time containing more than 10 g Nm^{-3} tars (phase **b**). The OCV (~850 mV) and voltage during current load (~785 mV) were both lower than during the tar-free operation period (phase **a**) because of a lower fuel inlet LHV of the non pre-reformed gas. For phase **c**, the OCV was ~840 mV and the cell voltage during the first 5 h of current load decreased slightly from 790 mV to 785 mV due to a decreasing wood gas LHV. Following 1 h of operation on the synthetic reference gas mixture (**R**) due to a gasifier interruption, the SOFC was fueled again with wood gas for another 2 h, resulting in an OCV around 833 mV and voltage under load increasing from 785 mV to 790 mV.

The control of the cell temperature was difficult and slow due to the thermal inertia of the massive ceramic parts of the cell housing and tubing. When changing from the reference gas mixture to wood gas with much higher flow and very high steam content, the measured cell temperature at the fuel inlet initially suddenly dropped by ~50 °C during phase **a**, and by almost 80 °C during phases **b** and **c** due to the highly endothermic reforming reactions of methane and possibly other hydrocarbons occurring during the operation on non pre-reformed wood gas. The resulting average cell temperatures were 853 °C for phase **a**, 839 °C for phase **b** and 848 °C for phase **c**. Initial OCV on the synthetic reference gas operation (~1008 mV at 857 °C) was higher than after phase **a** (~999 mV at 877 °C) and phase **b** (~987 at 905 °C) which can partly be attributed to the inverse relation of Nernst potential with temperature. Another influencing factor was the increasing ambient temperature over the test day due to the heat rejection of all the experimental equipment, which caused slightly higher humidification of the synthetic reference gas mixture (the humidifier always operated at room temperature) and thus

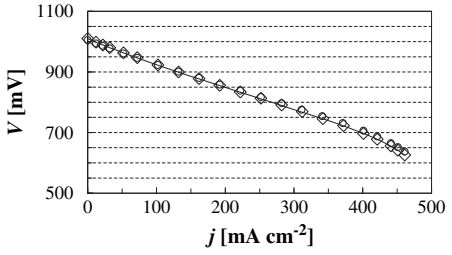

Fig. 6 – Voltage vs. current density (V–j) curves measured on H_2/N_2 reference gas R before phase a (open diamonds), after phase b (open circles) and after phase c (solid line).

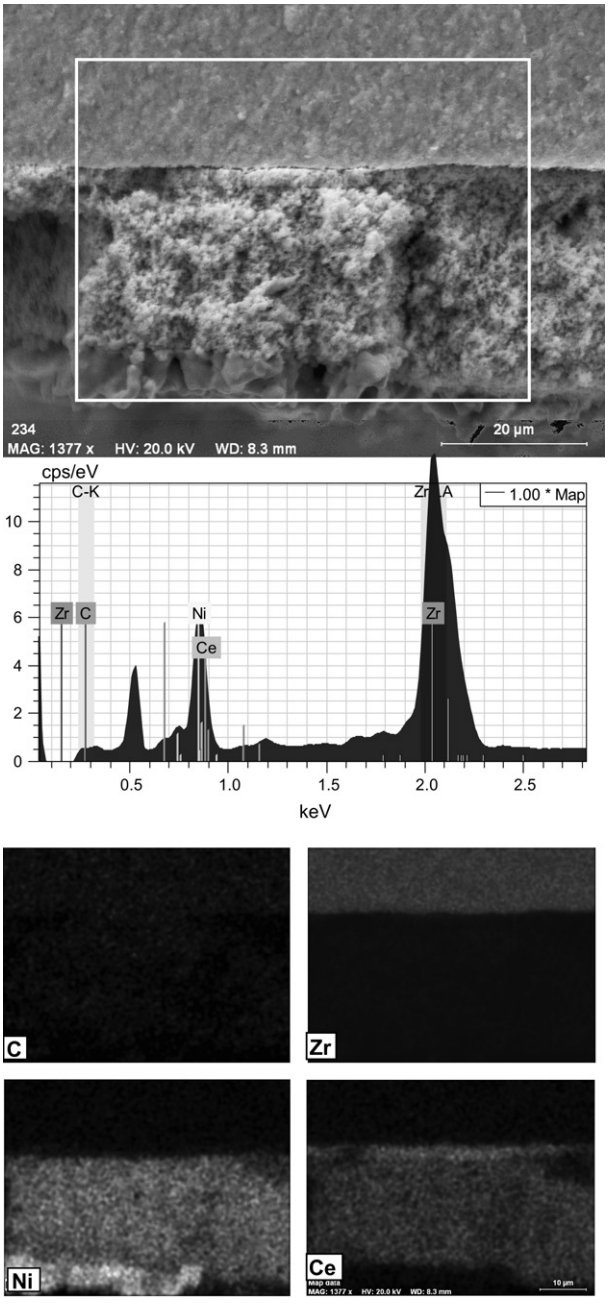

Fig. 7 – SE micrograph, EDS spectrogram and elemental mapping for carbon (C), zirconium (Zr), nickel (Ni) and cerium (Ce) of a sample from the tested cell.

further decreased the Nernst potential. The same explanations also account for the observation made during phase **c**.

Comparison of SOFC performance by means of *V–j* curves measured on the synthetic reference gas mixture before phase **a** and after phases **b** and **c** shows, that the cell maintained its initial performance as shown in Fig. 6: the three curves coincide.

The current presented experimental results of stable SOFC operation on real heavily tar-laden biomass derived product gas are promising when compared with the findings reported from tests with synthetically introduced comparable tar loads [14] on similar anode material where the introduction of different tar levels, i.e. Naphthalene (0.29–6 g Nm^{-3}), Phenanthrene (1 g Nm^{-3}), Pyrene (0.2 g Nm^{-3}) caused a rapid voltage drop within a few hours before leveling out at a lower voltage.

3.5. *SEM-EDS analysis of the anode*

Post experimental examination of the SOFC membranes with SEM-EDS did neither reveal any carbon deposition, nor any contamination from impurities while the microstructure of the anode was found intact. Fig. 7 shows elemental EDS mapping of a sample from the employed cell. While the mapping of elements Ni, Zr and Ce, which are really present in the anode (Zr in the electrolyte), can be clearly distinguished, the mapping of carbon C is distributed homogeneously over the whole analysis area (also over the electrolyte indicated by Zr). These carbon counts are attributed to noise (and due to carbon sputtering used in the SEM technique) as there is also no detectable peak for carbon in the EDS spectrogram.

4. Conclusions

The concept of biomass gasification coupling to SOFC has been predominantly studied in theory. Previous experimental efforts mostly concerned simulated product gas experiments from bottled gases. In this work actual high-tar laden producer gas from a 100 kW_{th} circulating fluidized bed gasifier was fed to a commercially available planar SOFC with a Ni-GDC anode. Hot gas cleaning was adopted for this effort.

The short-term operation (~7 h) on a high tar load (>10 g Nm^{-3}) has proven that tars did not cause immediate problems to Ni-GDC anode operation. Indeed, no performance loss was observed and no carbon or other product gas trace constituents contamination of the anodes was found when the SOFC membranes were examined with SEM/EDS after the tests. The difference in cell voltage output, i.e. slightly smaller for operation on non pre-reformed wood gas, is attributed to the difference in the lower heating value of the wood gas entering the SOFC: the LHV is higher for the pre-reformed wood gas and thus results in higher initial Nernst potential. Furthermore, short periods of H_2S breakthrough (<1.5 ppmv for less than 2 h during test phase **c**) did not influence SOFC performance.

In the future detailed experimental studies are required to clearly understand the influence of heavy tars on SOFC operation when fed with biosyngas and to identify safe operating conditions for SOFCs when fed with tar-laden biosyngas.

Acknowledgements

The investigations were supported by the European Commission within the 6th Framework Program (STREP Bio-Cellus, Biomass Fuel Cell Utility System, Contract No: 502759). The authors would also like to thank Dr. W. de Jong for his support during the experimental campaign.

REFERENCES

[1] Milne TA, Abatzoglou N, Evans RJ. Biomass Gasifier 'Tars': their Nature, Formation and Conversion, NREL Technical Report (NREL/TP-570-25357); 1998.
[2] Eg & G Technical Services Parsons Inc., Science Applications International Corporation. Fuel cell handbook. 5th ed. Morgantown, WV: US Department of Energy, Office of Fossil Energy, National Energy Technology Laboratory; 2000.
[3] Norheim A, Wærnhus I, Brostrom M, Hustad JE, Vik A. Experimental Studies on the Influence of H_2S on solid oxide fuel cell performance at 800 °C. Energy Fuels 2007;21:1098–101.
[4] Aravind PV, Ouweltjes JP, Woudstra N, Rietveld G. Impact of biomass-derived contaminants on SOFCs with Ni/Gadolinia-doped ceria anodes. Electrochem. Solid-State Lett. 2008;11: B24–8.
[5] Dekker N, Rietveld G. Highly efficient conversion of ammonia into electricity by solid oxide fuel cells. In: Proceedings of the sixth European solid oxide fuel cell forum, Lucerne, Switzerland; 28 June–2 July 2004.
[6] Singh D, Hernandez-Pacheco E, Hutton PN, Patel N, Mann MD. Carbon deposition in an SOFC fueled by tar-laden biomass gas: a thermodynamic analysis. J Power Sources 2005;142:194–9.
[7] Ormerod RM. In: Singhal SC, Kendall K, editors. High-temperature solid oxide fuel cells: fundamentals, design and applications. Oxford: Elsevier Science; 2003. p. 333–62.
[8] Wang W, Jiang SP, Yoong Tok AI, Luo L. GDC-impregnated Ni anodes for direct utilization of methane in solid oxide fuel cells. J Power Sources 2006;159:68–72.
[9] Huang TJ, Wang CH. Methane decomposition and self de-coking over gadolinia-doped ceria-supported Ni catalysts. Chem Eng J 2007. 10.1016/j.cej.2007.01.024.
[10] Huang TJ, Wang CH. Factors in forming CO and CO_2 over a cermet of Ni-gadolinia-doped ceria with relation to direct methane SOFCs. J Power Sources 2006;163:309–15.
[11] Suwanwarangkul R, Croiset E, Entchev E, Charojrochkul S, Pritzker MD, Fowler MW, et al. Experimental and modelling study of solid oxide fuel cell operating with syngas fuel. J Power Sources 2006;161:308–22.
[12] Baron S, Brandon N, Atkinson A, Steele B, Rudkin R. The impact of wood-derived gasification gases on Ni-CGO anodes in intermediate temperature solid oxide fuel cells. J Power Sources 2004;126:58–66.
[13] Ouweltjes JP, Aravind PV, Woudstra N, Rietveld G. Biosyngas utilization in solid oxide fuel cells with Ni/GDC anodes. In: Proceedings of the First European Fuel Cell Technology & Applications Conference, Rome, Italy; December 14–16 2005.
[14] Dekker NJJ, Ouweltjes JP, van der Drift A, Rietveld G. Efficient conversion of biogas in electricity and heat by a solid oxide fuel cell. In: Proceedings of the 15th European biomass conference & exhibition, Berlin, Germany; May 7–11 2007.
[15] Oudhuis ABJ, Bos A, Ouweltjes JP, Rietveld G, van der Giesen AB. High efficiency electricity and products from biomass and waste; experimental results and proof of principle of staged gasification and fuel cells. In: Proceedings of the 2nd World

conference and technology exhibition on biomass for energy, industry and climate protection, Rome, Italy; May 10–14 2004.
[16] Nagel FP, Biollaz S, Jenne M, Stucki S. Link-up of a 1 kW SOFC with an updraft-wood gasifier via hot gas processing. In: Proceedings of the 15th European biomass conference & exhibition, Berlin, Germany; May 7–11 2007.
[17] Hofmann Ph, Schweiger A, Fryda L, Panopoulos KD, Hohenwarter U, Bentzen JD, et al. High temperature electrolyte supported Ni-GDC/YSZ/LSM SOFC operation on two-stage Viking gasifier product gas. J Power Sources 2007; 173:357–66.
[18] Hofmann Ph, Panopoulos KD, Fryda LE, Schweiger A, Ouweltjes JP, Karl J. Integrating biomass gasification with solid oxide fuel cells: effect of real product gas tars, fluctuations and particulates on Ni-GDC anode. Int J Hydrogen Energy 2008;33:2834–44.
[19] BioCellUS EU project website, www.biocellus.com, www.biocellus.de, www.biocellus.net.
[20] Siedlecki M, Simeone E, de Jong W, Verkooijen AHM. Characterization of gaseous and condensable components in the product gas obtained during steam-oxygen gasification of biomass in a 100 kW_{th} CFB gasifier. In: Proceedings of the 15th European biomass conference & exhibition, Berlin Germany; May 7–11 2007.
[21] Brage C, Yu Q, Chen G, Sjöström K. Use of amino phase adsorbent for biomass tar sampling and separation. Fuel 1997;76:137–42.
[22] Schweiger A, Hohenwarter U. Small scale hot gas cleaning device for SOFC utilisation of woody biomass product gas. In: Proceedings of the 15th European biomass conference & exhibition, Berlin Germany; May 7–11 2007.
[23] Karellas S, Karl J. Analysis of the product gas from biomass gasification by means of laser spectroscopy. Opt. Lasers Eng. 2007;45:935–46.
[24] Neeft JPA, Knoef HAM, Zielke U, Sjöström K, Hasler P, Simell PA, et al. Guideline for sampling and analysis of tar and particles in biomass producer gases, version 3.3. Energy project ERK6-CT1999-20002 (Tar Protocol).
[25] FactSageTm, ver. 5.4.1, www.gtt-technologies.de, www.factsage.com.